Effect of bentonite slurry on the function of foam for changing the permeability characteristics of sand under high hydraulic gradients

Fanlin Ling[1], Shuying Wang[2*], Qinxin Hu[3], Shuo Huang[4], Zhiyao Feng[5]

1 School of Civil Engineering, Central South University, Changsha, Hunan 410075, China. Email: lotusling@csu.edu.cn

2 School of Civil Engineering, Central South University, Changsha, Hunan 410075, China. (corresponding author). Email: sywang@csu.edu.cn

3 Department of Civil and Environmental Engineering, University of Strathclyde, Glasgow G1 1XJ, United Kingdom. Email: qinxin.hu@strath.ac.uk

4 College of Engineering, Peking University, Beijing, 100871, China. Email: huangshuolbdz@163.com

5 School of Civil Engineering, Central South University, Changsha, Hunan 410075, China. Email: fzy1124@126.com

Abstract

During earth pressure balance (EPB) shield tunnelling in sandy ground, not only foam but also other conditioning agents need to be injected to reduce the permeability of muck and avoid water spewing out of the screw conveyor. Permeability tests were carried out to study the permeability characteristics of conditioned sand under high hydraulic gradients. A low bentonite slurry injection ratio (*BIR*) enhanced the workability of foam-conditioned sand. As the hydraulic gradient increased, the initial permeability coefficient of conditioned sand increased, and the initial stable period became shorter or disappeared. The *BIR* had a more significant effect on the permeability of conditioned sand than the foam injection ratio (*FIR*), and this effect gradually weakened as the hydraulic gradient increased. The initial permeability coefficient of the foam-bentonite slurry-conditioned sand decreased by approximately an order of magnitude compared with that of the foam-conditioned sand. With the addition of bentonite slurry, suitable sand conditioning can accept a higher water content (*w*) and lower *FIR*, resulting in suitable ranges of *w* and *FIR* that are more flexible. Finally, the mechanism of stabilizing foam under the action of bentonite slurry was discussed by considering the interaction between foam bubbles and fine particles.

Keywords

sand conditioning, foam, bentonite slurry, permeability, hydraulic gradient

1 Introduction

Spewing water and excavation face instability easily occur during earth pressure balance (EPB) shield tunnelling in water-rich sandy ground (Psomas 2001; Budach and Thewes 2015; Borio and Peila 2010; Bezuijen 2012). Soil conditioning is an effective way to solve this problem; agents are injected into the muck before the cutterhead and in the excavation chamber, which causes the muck to become pulpy (Vinai et al. 2008). In this state, the muck has suitable fluidity, low permeability, suitable compressibility and a low internal friction angle (Thewes and Budach 2010; Langmaack and Lee 2016; Mori et al. 2017; Liu et al. 2018). In general, to prevent water spewing, the permeability coefficient of the conditioned muck should be less than 10^{-5} m/s and maintained for at least 90 min (Quebaud et al. 1998; Borio and Peila 2010; Budach 2012; Budach and Thewes 2015; Wang et al. 2020). Foam, bentonite slurry and polymers are often used as single or combined agents to condition the muck.

Foam is widely used in sandy soils due to its advantages of convenient preparation, low cost, and dissipation after tunnel construction (Langmaack and Lee 2016; Mori et al 2018). Some scholars have studied the permeability characteristics of foam-conditioned sand. Bezuijen et al. (1999) pointed out that the permeability of conditioned sand is closely related to the filling state of sand pores by foam. The better the foam fills in the pores, the lower the permeability coefficient of foam-conditioned sand. Borio and Peila (2010) carried out constant head permeability tests under different water pressures to study the permeability of foam-conditioned sand and found that the permeability coefficient of foam-conditioned sand decreased with an increase in the foam injection ratio (*FIR*, which is defined as the ratio of the volume of foam to that of a soil specimen in the natural loose

state) but increased with an increase in the foam expansion ratio (*FER*, which is defined as the ratio of the volume of foam to that of foam solution) and water pressure. However, because foam is a metastable multiphase system with an uneven bubble size (Pitois et al. 2009; Rouyer et al. 2014), the permeability of foam-conditioned sand has a certain temporal variability; that is, the permeability coefficient (k) is maintained at a low level in the initial period; however, as the foam bubbles continue to dissipate and are flushed out over time, k increases rapidly, and after a fast growth period, it finally stabilizes (Budach 2012; Hu et al. 2020; Wang et al. 2021). Hu et al. (2020) studied the effect of hydraulic gradients on the permeability characteristics of foam-conditioned sand. When the hydraulic gradient was high, the permeability coefficient of the muck did not meet the requirement of a low permeability coefficient, necessitating the selection of other agents or combined conditioning considerations. This is consistent with the experimental results of Borio and Peila (2010) and Peila (2014). Huang et al. (2019) found that when an EPB shield was tunnelled in water-rich sandy soils and conditioned only by foam, the permeability coefficient of the muck increased as the effective particle size (d_{10}) increased, and the temporal variation in the permeability coefficient increased. When the sand had a low fine particle percentage, they suggested adding other agents, such as bentonite slurry. Quebaud et al. (1998) found that soil that was too coarse or too fine could not be well conditioned with foam, and other agents needed to be added. Jancsecz et al. (1999) pointed out that the foam-bentonite slurry combination produced better conditioning states of sandy soils. When the foam-bentonite slurry combination was used for muck conditioning, the ground surface settlement was significantly reduced, and the supporting pressure of the excavation face maintained stability.

In summary, previous studies have mainly focused on the permeability characteristics of foam-conditioned soil. However, at the same time, many studies have shown that using only foam as a single agent does not meet the requirements of low permeability for EPB shield tunnelling, especially when EPB shields re-thrust after a long standstill or tunnel in sandy ground under high water pressure. Adding other agents to consider combined conditioning, especially foam-bentonite slurry combinations, is necessary (Hajialilue-Bonab et al. 2014; Huang et al. 2019; Hu et al. 2020). However, there are few studies on the permeability characteristics of soil conditioned with foam and bentonite slurry.

This study is a supplement to Hu et al. (2020), who reported that the permeability coefficient of foam-conditioned sand with high water content was too high. A series of large-scale permeability tests were carried out in this study on foam-bentonite slurry-conditioned sand to investigate the effect of bentonite slurry on the function of foam for changing the permeability characteristics of sand under high hydraulic gradients. The permeability mechanism of muck with foam-bentonite slurry combined conditioning was analysed from the point of view of the interaction between foam (metastable structure) and bentonite (fine soil particles). The permeability and workability of foam-bentonite slurry-conditioned sand and those of foam-conditioned sand were compared and discussed, and the superiority of sand conditioned with foam and bentonite slurry was shown.

2 Background

Although it is recommended that EPB shields should be used with a hydrostatic pressure head of less than 20 m (Galli and Thewes 2014), the hydrostatic pressure head in some EPB tunnel projects is higher than 20 m when tunnelling in deep granular strata or under rivers due to a relatively

low engineering cost with EPB shields. For example, the Longquan water tunnel in the Dianzhong Water Diversion Project of China is being constructed with an EPB shield, and the maximum hydrostatic pressure head reaches more than 50 m (the maximum burial depth is 75 m). Therefore, studying the permeability characteristics of conditioned sand under high hydraulic gradients is significant for guiding the safe excavation of EPB shields under special geological conditions in the future.

Hu et al. (2020) used the slump test to evaluate the workability of foam-conditioned sand. Studies have suggested that the appropriate slump value is 15-20 cm (Vinai et al. 2008; Wang et al. 2020), and the conditioning states of sand were classified into five categories: insufficient conditioning, suitable conditioning without any water or foam bleeding, suitable flowability but with water bleeding, excessive conditioning with water bleeding, and excessive conditioning with probable foam bleeding. The water bleeding phenomenon conveys that water flows out of soil when it exists as free water in the soil, whereas probable foam bleeding means that foam flows out of soil when it cannot be sufficiently locked by soil. During shield tunnelling, the conditioned sand must maintain relatively suitable workability to be discharged out of the shield chamber; therefore, the insufficiently conditioned sand was not studied here, so its permeability characteristics were not tested. With the exception of insufficient conditioning, four other above defined states of sand were used to investigate the permeability. Hu et al. (2020) found that with suitable conditioning without any water or foam bleeding and excessive conditioning with probable foam bleeding, the initial permeability coefficient of sand conditioned with foam was lower than 10^{-5} m/s when the hydraulic gradient was 2.67. However, the sand could not meet the permeability requirements (in which the

initial permeability coefficient of sand is lower than 10^{-5} m/s and maintained for more than 90 min) in the range of hydraulic gradients from 4 to 17 under suitable conditioning but with water bleeding and excessive conditioning with water bleeding. Fig. 1 shows the suitable sand conditioning parameters indicated by the squares "□" according to the slump tests. In Fig. 1, suitable conditioning parameters for sand with ideal permeability characteristics for different hydraulic gradients are also circled. As the hydraulic gradient increased, the conditioning parameters with suitable permeability characteristics transitioned to having a lower water content (w) and higher *FIR*, as shown by the arrow. When the hydraulic gradient was 11, the sand did not have suitable workability, although there were still some conditioning states that could meet the permeability requirements. When the hydraulic gradient reached 17, the sand under any conditioning state could not meet the requirements of low permeability. Among them, sand under the states of suitable conditioning but with water bleeding and excessive conditioning with water bleeding had a high moisture content. Excessive free water occupied the permeation channel, and the internal permeation channel of the soil could not be evenly filled with foam bubbles to form effective water-blocking structures. Once the permeability test began, the foam bubbles were quickly flushed away under hydrodynamic action, leading to the destruction of water-blocking structures, so the conditioning states were poor.

The mixture of bentonite and sand is often used to reduce the permeability of soil (Chapuis 1990; Sivapullaiah et al. 2000; Ma et al. 2020). Kenney et al. (1992) pointed out that the permeability coefficient of the sand/bentonite mixture depends on the properties of the bentonite. In the bentonite/sand mixture, sand forms a load-supporting framework, which enables the mixture to

achieve macroscopic stability. The hydration bentonite particles occupy the space between sand particles and can act as a seepage barrier. However, only using bentonite to condition the soil for EPB shield tunnelling in sandy ground is not enough. As heat is generated by the friction of the cutters, the bentonite/sand mixtures easily adhere to the cutterhead and cutters to cause clogging, thus reducing the efficiency of excavation. Therefore, the addition of foam is necessary for lubrication. Because sand cannot meet the permeability requirements at each hydraulic gradient when w=10%, FIR=10% and w=10%, FIR=20%, bentonite slurry was added to investigate the permeability of the conditioned sand. It is hoped that the sand conditioned with a combination of foam and bentonite slurry can maintain a lower permeability coefficient during EPB shield tunnelling in water-rich sandy ground. On the basis of the explanation of the mechanism of combined conditioning, this paper provides more conditioning parameters for sand conditioning.

3 Test methods

3.1 Test materials

The sand used in the tests was the same as that studied by Hu et al. (2020) and collected from the Xiangjiang River, Changsha, China. The soil was sieved, and the desired soil was prepared to have the same grain size distribution as that studied by Hu et al. (2020) in Fig. 2. The fine particles (<0.075 mm in diameter) comprised 0.08% of the soil, and the sand (0.075-4.75 mm in diameter) and gravel (4.75-75 mm in diameter) particles comprised 67.87% and 32.05% of the soil, respectively. According to ASTM D2488-17ε1 (ASTM 2017), the soil is classified as poorly graded sand (SP). Its specific gravity and minimum dry density were 2.634 and 1.74 g/cm^3, respectively, and the maximum porosity of the sand was calculated as 0.340.

A foam agent for EPB shield tunnelling with a weight concentration of 3% was used for the tests, and the major chemical compositions of the foam agent used are listed in Table 1. The foam generation system followed the requirements of the European Federation for Specialist Construction Chemicals and Concrete Systems (EFNARC 2005), as shown in Hu et al. (2020). Under the action of compressed air, the foam solution and air were evenly mixed in the foam generator, and the generated foam was collected at the outlet of the measuring plate. The *FER* was 10, and the half-life duration of the generated foam was approximately 6 min.

Sodium bentonite powder was used, and the bentonite slurry was prepared following the standard by ISO 13500: 2008(E) (the International Organization for Standardization). Powdered sodium bentonite was tested by X-ray diffraction (XRD) and the minerals of the specimen are listed in Table 2. Viscosity is an important performance index of the slurry. If the viscosity of the bentonite slurry is too high, its pumpability is poor, and it easily causes conditioning pipeline blockage. However, if the viscosity is too low, the slurry does not achieve a suitable conditioning function of the sand. Slurry viscosity was measured using a Marsh funnel (API 2009; Peila et al. 2011; Xu and Bezuijen 2018a). The bentonite slurry used in this study had a weight concentration of 7%, its fermentation time was 18 h, and the corresponding Marsh funnel viscosity was approximately 45 s.

3.2 Test equipment and approaches

The slump test was carried out to investigate the workability of the conditioned sand following ASTM C143/C143M-20 (ASTM 2020). The conditioned sand was poured into the standard slump cone, and then the cone was lifted vertically. The falling distance of the sand specimen was recorded, and the overall workability of the sand was analysed. A self-designed, large-scale permeameter that

followed the requirements of ASTM D2434-19 (ASTM 2019) was used to conduct the constant head permeability tests. The permeameter was 30 cm in diameter and 75 cm in height. Two porous plates were placed at the top and bottom of the sand specimen to prevent the movement of fine particles. For more details, please refer to Hu et al. (2020).

The permeability tests followed ASTM D2434-19 (ASTM 2019). Each test was carried out according to the following steps.

(1) The sand was mixed with water for 1 min and left to stand to ensure that the sand specimen could fully absorb the water. Then, the bentonite slurry was mixed with sand for 1 min in a concrete mixer. Subsequently, the foam was added and stirred together for 1 min to prepare the conditioned sand.

(2) Filter paper was placed on the bottom plate, and then the foam-bentonite slurry-conditioned sand was filled layer by layer into the permeameter; the total height of the specimen was approximately 60 cm. To prevent the possible influence of gravity on the density of the sand, each layer was poured gently onto the surface of the previous layer.

(3) The top plate was assembled, and the required hydrostatic pressure head was provided by changing the head of the water tank. Then, tap water was slowly supplied to the top of the specimen. Meanwhile, the air release valve was opened.

(4) After the permeameter was full of water, the air release valve was closed, and one-dimensional permeation downward along the axis of the permeameter was conducted. The whole process of specimen preparation for each permeability test was conducted in approximately 25 min.

(5) The height of sample l (m) in different time periods (which changed due to foam dissipation

and specimen compression), the volume of the seepage quantity Q (m^3), the water pressure P_t (m) at the top gauge and the water pressure P_b (m) at the bottom gauge in a given period of time Δt were recorded. The permeability coefficient k at different times was calculated by Darcy's law, as reported in Hu et al. (2020). When the permeability coefficient increased slowly and even remained with time, the permeability test was halted.

The conditions of the permeability tests are shown in Table 3.

4 Results of the slump tests

The muck discharged by the screw conveyor is required to have appropriate workability, which has often been evaluated based on slump values for EPB shield tunnelling (Peila 2014; Budach and Thewes 2015). Fig. 3 shows the results of the slump tests. It should be noted that the data for the dotted line, that is, the slump values of foam-conditioned sand, are from Wang et al. (2020).

According to Fig. 3, the slump values were generally high and increased with increasing *FIR* for the sand conditioned only with foam. Especially when the *FIR* was greater than 10%, the sand was in an excessive conditioning state with high fluidity, and its slump value exceeded the ideal range of 15-20 cm (Vinai et al. 2008; Wang et al. 2020). With the addition of a small amount of bentonite slurry (*BIR*=5%), the workability was improved, and the slump value was significantly reduced. For example, with a constant *w*=10% and *FIR*=10%, the slump values were 19.9 cm and 18.0 cm, respectively, with *BIR*=0% and *BIR*=5%. The bentonite slurry can fill the pores between the coarse particles and cement the fine particles in the specimen (Xu and Bezuijen 2018b). Therefore, sand has better water retention and certain cohesion, which is conducive to the control of muck discharging, to better control the stability of the excavation face for EPB shield tunnelling.

However, a higher *BIR* is not necessarily better. The slump value of the combined conditioned sand increased to be close to that of the foam-conditioned sand when the *BIR*=10%. The reason is that if the *BIR* greatly increases, the excess bentonite slurry dominates the conditioned sand and reduces its shear strength better than the foam-bentonite slurry mixture.

5 Results of the permeability tests

5.1 Permeability characteristics of foam-bentonite slurry-conditioned sand

Fig. 4 shows the time-varying curves of the permeability coefficients (k) of foam-bentonite slurry-conditioned sand. Similar to foam-conditioned sand (Huang et al. 2019; Hu et al. 2020), there were three main periods of permeability coefficients, including an initial stable period, a fast growth period and a slow growth period. Under hydrodynamic action, foam bubbles and bentonite particles constantly adjusted their positions in the soil skeleton to form the most effective water-blocking structures. Therefore, during the early stage of the permeability test, the permeability coefficient showed a certain short-term reduction as shown in Fig. 5, which is the expanded inset of the early stage of the permeability coefficient in Fig. 4. After the foam bubbles and bentonite particles were stabilized under the seepage forces in the soil, the permeability coefficient of less than 10^{-5}m/s in the initial stable period remained more than 90 min in most cases, as shown in Fig. 4. During this period, the permeability coefficient was maintained at a low level. The length of the initial stable period was related to the *FIR* and *BIR*. When the *FIR* was constant, it extended with the increase in the *BIR*, and when the *BIR* was constant, it extended with the increase in the *FIR*. As shown in Fig. 4a, when the hydrostatic pressure head (P)=1.9 m and w=10%, the initial stable period extended from 932 min to 1200 min with an increase in the *FIR* from 10% to 20% and a constant *BIR*=5%,

but it increased from 932 min to 1626 min with an increase in the *BIR* from 5% to 10% and a constant *FIR* =10%. Thus, the *BIR* had a more significant effect on the initial stable period than the *FIR*. The same effect could be observed in Fig. 4b-d. After the initial stable period, the foam continued to coarsen, dissipate or be flushed out by water, forming a larger number of permeation channels in the conditioned sand and resulting in a rapid increase in the permeability coefficient; the sand thus entered the fast growth period. Finally, after a large number of foam bubbles dissipated or were flushed out of the specimen, the permeation channels tended to be stable, and the growth rate of the permeability coefficient slowed down, making the sand enter a slow growth period.

Additionally, with an increase in the hydrostatic pressure head (*P*) from Fig. 4(a) to Fig. 4(b), the permeability coefficient of foam-bentonite slurry-conditioned sand changed rapidly, showing that the initial stable period was shortened, the growth rate of the fast growth period was increased, and the slow growth period occurred sooner than expected. When *w*=10%, *FIR*=10%, and *BIR*=10%, the initial stable periods of the conditioned soil were 1626 min, 1104 min, 465 min and 100 min at hydrostatic pressure heads of 1.9 m, 2.9 m, 5.6 m and 9.6 m, respectively. When *w*=10%, *FIR*=10%, and *BIR*=5%, there was no initial stable period at a hydrostatic pressure head of 9.6 m. The reason is that with an increase in *P*, the water pressure acting on the conditioned soil increased and the water flow rate increased. Even if there are bentonite particles filling the sand, the foam bubbles filling the pores between the soil particles are likely to lose stability and are then flushed away by water, forming a larger number of permeability channels, and the permeability coefficient increases rapidly. For example, when *w*=10%, *FIR*=10%, and *BIR*=5%, the growth rate of the permeability coefficient was approximately 4.93×10^{-7} m/s per hour in the fast growth period at a *P* of 1.9 m, and

when the P increased to 2.9 m, 5.9 m and 9.6 m, the growth rates of the permeability coefficient were 6.62×10^{-7} m/s, 1.11×10^{-6} m/s and 1.19×10^{-6} m/s per hour, respectively.

At a constant P and *FIR*, the growth rate of the permeability coefficient slowed with an increasing *BIR*. As a highly viscous fluid, the bentonite slurry can tightly wrap particles in the sand, fill the pores in the sand, and reduce the permeability coefficient of the sand. On the other hand, fine bentonite particles are adsorbed at the air-liquid interface of foam bubbles, increasing the flow resistance of water on the foam film (Zhao et al. 2016; Guillermic et al. 2009). In addition, the existence of bentonite particles on the foam film and the permeability channels parallel to the surface of the foam film hinder air exchange between foam bubbles, slowing down the coarsening and dissipation of foam (Erasov et al. 2015). For example, with P=1.9 m, w=10%, and *FIR*=10%, the growth rate of the permeability coefficient decreased from 4.93×10^{-7} m/s to 4.08×10^{-7} m/s per hour for sand with an increase in the *BIR* from 5% to 10%. Note that the addition of fine particles could only slow but not prevent foam from coarsening and dissipating (Louvet et al. 2010).

5.2 Effect of the hydraulic gradient on the permeability characteristics of foam-bentonite slurry-conditioned sand

By changing the hydrostatic pressure head (P), permeability tests under different hydraulic gradients were carried out on sand specimens with different conditioning parameters. The variations in the duration of the initial stable period (t_s), the initial permeability coefficient (k_i), and the permeability coefficient in the slow growth period (k_{sg}) against the hydraulic gradient were investigated. k_i is used as the mean value of the permeability coefficient during the whole initial stable period, and k_{sg} is determined to be the permeability coefficient at the intersection point of the fast and slow growth periods.

Fig. 6 shows the relationship between the duration of the t_s and hydraulic gradient (i) of the foam-bentonite slurry-conditioned sand. The duration of the initial stable period of the permeability coefficient decreased with an increase in the hydraulic gradient, and the slope of the curve tended to be flat, indicating that the decreased rate of t_s further decreased along the hydraulic gradient. According to Darcy's law, the water flow rate increased with an increase in the hydraulic gradient, and the disturbance of the seepage force action on the foam structure was aggravated so that the foam bubbles in conditioned sand were more fragile, resulting in the destruction of water-blocking structures and a decrease in t_s. For example, with w=10%, FIR=20%, and BIR=10%, when the hydraulic gradient increased from 4.01 to 5.77, t_s decreased from 1950 min to 1398 min, decreasing by approximately 313.6 min per unit hydraulic gradient; when the hydraulic gradient increased from 11.3 to 17.5, t_s decreased from 626 min to 152 min, decreasing by only 76.5 min per unit hydraulic gradient. When the hydraulic gradient increased to a certain extent, most permeation channels blocked by foam were rapidly penetrated. Thus, only a small number of foam bubbles in the soil pores could maintain stability, and the range in which t_s could decline also decreased. Compared with the conditioning parameters of w=10%, FIR=20%, and BIR=5% and w=10%, FIR=20%, and BIR=10%, with the increase in the BIR, t_s increased in each hydraulic gradient. More bentonite particles filled pores, thereby increasing the fine particles of the specimen; at the same time, they were also adsorbed on the foam film, thereby forming more compact structures. They could fill permeation channels, impede film drainage and air exchange between foam bubbles, delay the foam dissipation rate and improve foam stability (Horozov 2008).

Fig. 7 shows the relationship between k_i and the hydraulic gradient of the foam-bentonite slurry-

conditioned soil. When the hydraulic gradient was low, k_i grew slowly. For example, when w=10%, FIR=10%, and BIR=5% and the hydraulic gradient increased from 4.2 to 10.9 (approximately 2.6 times), k_i increased from 1.74×10^{-6} m/s to 2.64×10^{-6} m/s (only 1.5 times). With an increase in the hydraulic gradient, the growth rate of k_i increased gradually. When w=10%, FIR=10%, and BIR=5% and the hydraulic gradient increased from 10.9 to 18.0 (approximately 1.7 times), k_i increased from 2.64×10^{-6} m/s to 6.94×10^{-6} m/s (approximately 2.6 times). Additionally, the BIR changed the influence of the hydraulic gradient on k_i to some extent. Under high hydraulic gradients (higher than 10.0), the BIR increased from 5% to 10%, and the growth rate of k_i slowed significantly.

Fig. 8 shows the relationship between the permeability coefficient in k_{sg} and the hydraulic gradient of the foam-bentonite slurry-conditioned soil. As the hydraulic gradient increased, k_{sg} decreased gradually, and the slope of the curve showed that the rate of the decrease in k_{sg} slowed down. For example, when w=10%, FIR=20%, and BIR=5%, the hydraulic gradient increased from 3.9 to 17.2, and k_{sg} decreased from 2.35×10^{-5} m/s to 2.12×10^{-5} m/s, a decrease of 10%. The k_{sg} decreased because the foam bubbles almost dissipated or flushed out, and the permeability was dominated by the soil itself. As the hydraulic gradient increased, a seepage-induced consolidation process occurred in the soil. Fox (1996) also pointed out that using high hydraulic gradients would lead to a decrease in the permeability coefficient, especially for soils with a high compressibility, such as soft clays and soil-bentonite slurries. The process of increasing the hydraulic gradient also causes the migration of fine particles, which may be trapped downstream of the soil specimen (Olson and Daniel 1981; Leonards et al 1991). The fine bentonite particles were closely arranged, which blocked permeation channels and pores, resulting in a decrease in the permeability coefficient at the

bottom of the permeameter. However, due to the scale limitation of sand specimen tested in laboratory, it should be noted that the test results can be used as a useful indicator, but do not necessarily represent field behaviour.

6 Discussion

6.1 Comparative study on the permeability of foam-bentonite slurry-conditioned sand and foam-conditioned sand

According to the research results of Hu et al. (2020), using only foam to condition sand does not fully meet the permeability requirements of engineering for EPB shield tunnelling under high hydraulic gradients. Especially for the specimens with high water contents (w=10%, FIR=10% and w=10%, FIR=20%), the initial permeability coefficients of foam-conditioned sand did not meet the requirements of $k_i \leq 10^{-5}$ m/s and $t_s \geq 90$ min at the four hydrostatic pressure heads of 1.9 m, 2.9 m, 5.6 m and 9.6 m. On this basis, foam and bentonite slurry were used together to condition the sand with the same grain gradation as that in Hu et al. (2020). The time-varying curve comparison of the permeability coefficient is shown in Fig. 9, where the dotted line data are from Hu et al. (2020), and the solid line represents the upper limit of the ideal permeability coefficient of 10^{-5} m/s for EPB shield tunnelling.

The dotted line in Fig. 9 shows that the permeability coefficient of the conditioned soil with a high water content (w=10%) was high at each hydrostatic pressure head (P) when only foam was used as a conditioning agent, and the time-varying curves of the permeability coefficient had no initial stable period. The initial permeability coefficient far exceeded the upper limit of 10^{-5} m/s, and the growth rate was high in the fast growth period. Comparing the sand specimens with conditioning parameters of w=10%, FIR=20%, and BIR=0% and w=10%, FIR=20%, and BIR=5%,

the latter had a longer initial stable period than the former. The foam-bentonite slurry-conditioned sand had a lower permeability coefficient and a lower growth rate than those of the foam-conditioned sand in the same permeability period. The initial permeability coefficient of the combined conditioned sand was approximately 1/10 of that of the foam-conditioned sand. The foam-bentonite slurry combined conditioning satisfied the permeability requirements of the muck (i.e., the initial permeability coefficient of sand was lower than 10^{-5} m/s and maintained for more than 90 min), but the single foam conditioning did not. Fig. 9 shows that under high hydraulic gradients, foam bubbles easily became unstable, leading to the destruction of the water-blocking structures. As a result, permeation channels were completely connected, and the permeability coefficient increased rapidly. To some extent, the bentonite slurry provided more fine particles for the sand specimen and effectively filled pores between the coarse particles. Simultaneously, the aggregation of fine bentonite particles increased the viscosity of the liquid phase, and the stability of the foam was promoted. The bentonite particles and foam bubbles jointly formed water-blocking structures to maintain the low permeability of the conditioned sand.

According to Fig. 1, reasonable conditioning for foam-conditioned sand should be carried out in the direction of a lower w and higher FIR, and the reasonable conditioning zone becomes gradually smaller with a higher hydraulic gradient. After the bentonite slurry is added, the amount of foam needed for suitable conditioning states is reduced. The bentonite slurry also enhances the water retention of the conditioned sand, resulting in sand conditioning with foam accepting a higher water content to obtain a suitable permeability state. In Fig. 1, sand conditioning with w=10% and FIR=10% conditions cannot satisfy the permeability requirements under a hydraulic gradient that is

less than 4. However, with the addition of bentonite slurry (*BIR*=5%), sand conditioning with the same *w* and *FIR* can still meet the permeability requirements under a hydraulic gradient as high as 17. The reasonable conditioning zone expanded in the direction of a higher *w* and lower *FIR* with the addition of bentonite slurry.

6.2 Stabilizing mechanism of foam by bentonite particles

Foam can be considered a porous medium containing permeation channels between foam bubbles, known as plateau channels (Rouyer et al. 2014; Wang et al. 2020; Xu et al. 2021a). According to the Young-Laplace equation, the pressure in small foam bubbles was higher than that in large bubbles. With contact between small and large foam bubbles, the air in small bubbles entered the large bubbles through the foam film, and foam coarsening occurred. However, with the addition of bentonite slurry, fine bentonite particles occurred between the liquid film of the foam bubbles and formed a steric barrier to limit liquid film drainage to the plateau channels and prevent the foam from coarsening or dissipating (Erasov et al. 2015). Two mechanisms of stabilizing foam by bentonite particles are as follows.

On the one hand, the fine bentonite particles themselves need to be stabilized on the foam film to promote the stability of liquid between foam bubbles. The particle detachment energy (ΔG) is an important factor to describe the effect of fine particles on the stability of foam liquid (Kaptay 2006). The particle detachment energy is related to the free energy involved in removing the adsorbed particles from the foam film. When ignoring buoyancy and gravity, ΔG can be calculated by Equation (1) proposed by Hunter et al. (2008):

$$\Delta G=\pi R^2\sigma(1-cos\theta)^2 \quad (1)$$

where R is the particle radius, σ is the surface tension at the air-liquid interface, and θ is the particle

contact angle.

On the other hand, the bentonite particles should stabilize the foam film and separate the foam bubbles. This refers to the theory of capillary pressure, which suggests that the stabilization of foam depends mainly on the capillary pressure between bubbles (Horozov 2008). Another perspective is that the foam bubbles attempt to break the pore-clogging effect of bentonite particles in the sand. Capillary pressure (P_c) is defined as the difference between the pressure in the bubble (P_1) and the pressure in the liquid (P_2). Fig. 10 shows the bentonite particles residing between the foam films. During the drainage process, the foam forms a meniscus around the bentonite particles. Specifically, this is a surface area effect in which bentonite particles provide a greater surface area for foam bubbles to affiliate with. As drainage increases, the meniscus profile continues to curve, the liquid film thickness (H) decreases, and the capillary pressure increases. At the end of the drainage process, H tends to 0, the foam bubbles contact each other, and the bentonite particles lose the capability of stabilizing foam bubbles.

The maximum capillary pressure (P_c^{max}) can be calculated by Equation (2) proposed by Kaptay (2006):

$$P_c^{max} = \pm\, p \frac{2\sigma}{R} \cos\theta \tag{2}$$

where p is a theoretical parameter, which is a function of foam film coverage by particles.

The above two mechanisms can be used to explain the stability of the foam in conditioned sand under the action of bentonite. Equation (2) shows that P_c^{max} increases with decreasing θ and R, indicating more difficulty in the drainage of foam liquid and contacting foam bubbles. However, from Equation (1), ΔG decreases with decreasing θ and R, which is more beneficial for the drainage

of foam liquid and contact between foam bubbles. Therefore, the function of foam stabilization by fine particles is the best under optimal contact angle and particle size values.

Kaptay (2006) pointed out that the optimal contact angle for particles stabilizing foam bubbles is mainly distributed in the range of 70°~110°. The contact angle of bentonite is generally 70.82° (Chen et al. 2016). Therefore, bentonite can be an excellent option for stabilizing foam bubbles. However, the optimal particle size has not been determined. According to the test results of Wu et al. (2020) and Xu et al. (2021b), foam mixed with fine soil particles had a lower size growth rate than pure foam, and the foam bubbles could remain steady for a long time in the soil. For the permeability of conditioned sand, foam bubbles with longer periods exist without coarsening, and a lower value of the initial permeability coefficient can be maintained for a long time. Referring to the test results in Section 6.1, when the conditioning parameters were w=10% and FIR=10%, the sand had a high permeability coefficient and no initial stable period. In contrast, after adding bentonite slurry with BIR=5% to sand with foam, the sand had a low initial permeability coefficient of 6.94×10^{-6} m/s for approximately 40 min under a hydraulic gradient as high as 17.

7 Conclusion

Foam-conditioned sand cannot meet permeability requirements when the hydraulic gradient is high. Through permeability tests of foam-bentonite slurry-conditioned sand under different conditioning parameters, the effect of bentonite slurry on the function of foam in changing the permeability characteristics of sand under high hydraulic gradients was studied. The following conclusions can be drawn.

Adding a small amount of bentonite slurry to the sand with foam could effectively reduce the

slump value of the sand and allow the sand to have suitable workability. However, with a constant *FIR* and a greater increase in the *BIR*, the fluidity of the conditioned sand increased, leading to a higher slump value. Therefore, attention should be given to foam-bentonite slurry combined conditioning such that *BIR* is not too high.

Under seepage force action, the foam bubbles and bentonite particles constantly adjusted their positions and moved in the soil skeleton to form effective water-blocking structures. The permeability coefficient had a short decreasing process during the early stage of the permeability test. After foam bubbles and bentonite particles were stabilized in the sand, the permeability coefficient entered an initial stable period for a long time, during which the permeability coefficient was maintained at a low level. The duration of the initial stable period was related to the *FIR* and *BIR*. When the *FIR* was constant, it increased as the *BIR* increased; when the *BIR* was constant, it also increased as the *FIR* increased.

As the hydraulic gradient increased, the time-varying curves of the permeability coefficient of foam-bentonite slurry-conditioned sand quickly passed through the initial stable period and the fast growth period and entered the slow growth period earlier. The foam bubbles were more likely to be unstable, so the permeability coefficient increased continuously and grew increasingly faster. Interestingly, when the hydraulic gradient was higher, the permeability coefficient in the slow growth period decreased, mainly because the fine bentonite particles migrated downward under the action of water at the higher flow rate, resulting in a more complete sealing of permeation channels at the bottom of the specimen.

The permeability coefficient of foam-bentonite slurry-conditioned sand was much lower than

that of foam-conditioned sand by approximately one order of magnitude. In the foam-bentonite slurry-conditioned sand, the initial stability time of the permeability coefficient below its upper limit (10^{-5} m/s) was longer. After the bentonite slurry was added, reasonable conditioning could be carried out in the direction of a higher *w* and lower *FIR*, and the reasonable conditioning zone was enlarged.

The stabilizing mechanism of foam bubbles by bentonite particles was discussed with two mechanisms: the particle detachment energy and the maximum capillary pressure. Bentonite particles with a suitable contact angle can be an excellent option to stabilize foam bubbles in conditioned sand and extend the duration of the initial stable period of the permeability coefficient.

This study is a supplement to Hu et al. (2020), which shows that foam cannot effectively condition sand when the hydraulic gradient is high, and the permeability characteristics of foam-bentonite slurry-conditioned sand are investigated in depth. Foam bubbles in the excavation chamber dissipate during the standstill of the EPB shield, which leads to a decrease in the chamber pressure and the instability of the excavation face (Bezuijen and Dias 2017). After the addition of the bentonite slurry, foam bubbles existed for a longer time than before, a phenomenon that can better maintain the pressure of the excavation chamber. Sand can also meet the permeability requirements with the condition of foam and bentonite slurry, so the combination of foam and bentonite slurry can be regarded as an effective method of sand conditioning.

Acknowledgements

The financial support from National Outstanding Youth Science Fund Project of National Natural Science Foundation of China (No. 52022112) is acknowledged and appreciated. The authors are also grateful for the recommendations from Xibao Zhang and Zhenyu Gong in China Railway No. 5 Engineering Group Co., LTD.

Reference

API (American Petroleum Institute). 2003. Recommended practice standard procedure for Field Testing Water-Based Drilling Fluids, 13B-1, 3rd ed. Washington, DC, USA: American Petroleum Institute.

ASTM (American Society for Testing and Materials). 2017. Standard Practice for Description and Identification of Soils: ASTM D2488-17ε1. ASTM International, West Conshohocken, PA.

ASTM (American Society for Testing and Materials). 2019. Standard Test Method for Permeability of Granular Soils (Constant Head): ASTM D2434-19. ASTM International, West Conshohocken, PA.

ASTM (American Society for Testing and Materials). 2020. Standard Test Method for Slump of Hydraulic-Cement Concrete: ASTM C143/C143M-20. ASTM International, West Conshohocken, PA.

Bezuijen, A. 2012. Foam used during EPB tunnelling in saturated sand, parameters determining foam consumption. In Proceedings WTC 2012, pp. 267-269. Bangkok, Thailand.

Bezuijen, A. and Dias, T. G. S. 2017. EPB, chamber pressure dissipation during standstill. EURO: TUN 2017 - 4th International Conference on Computational Methods in Tunnelling and Subsurface Engineering, **1**: 225-231. Innsbruck, Austria.

Bezuijen, A., Schaminee, P. E. L. and Kleinjan, J. A. 1999. Additive testing for earth pressure balance shields. In Proceedings Twelfth European Conference on Soil Mechanics and Geotechnical Engineering, pp. 1991-1996. Amsterdam, Netherlands.

Borio, L. and Peila, D. 2010. Study of the permeability of foam conditioned soils with laboratory tests. American Journal of Environmental Sciences, **6**(4): 365-370.

Budach, C. 2012. Untersuchungen zum erweiterten Einsatz von Erddruckschilden in grobkörnigem Lockergestein (Transl.: Investigations for extended use of EPB Shields in coarse-grained soils). PhD. thesis. Ruhr-Universität Bochum.

Budach, C. and Thewes, M. 2015. Application ranges of EPB shields in coarse ground based on laboratory research. Tunnelling and Underground Space Technology, **50**: 296-304.

Chapuis, R. P. 1990. Sand–bentonite liners: predicting permeability from laboratory tests. Canadian Geotechnical Journal, **27**(1): 47-57.

Chen, H., Li, Y., Zhou, Y. and He, J. 2016. Organic modification and characterization of Na-montmorillonite. (In Chinese). Journal of Wuhan University of Technology, **38**(3): 36-40.

EFNARC. 2005. Specification and guidelines for the use of specialist products for mechanised tunnelling (TBM) in soft ground and hard rock.

Erasov, V. S., Pletnev, M. Y. and Pokidko, B. V. 2015. Stability and rheology of foams containing microbial polysaccharide and particles of silica and bentonite clay. Colloid Journal, **77**(5): 614-621.

Fox, P. J. 1996. Analysis of hydraulic gradient effects for laboratory hydraulic conductivity testing. Geotechnical Testing Journal, **19**(2): 181-190.

Galli, M., and Thewes, M. 2014. Investigations for the application of EPB shields in difficult grounds. Geomechanik Und Tunnelbau, **7**(1): 31-44.

Guillermic, R. M., Salonen, A., Emile, J., and Saint-Jalmes, A. 2009. Surfactant foams doped with laponite: unusual behaviors induced by aging and confinement. Soft Matter, **5**(24): 4975-4982.

Hajialilue-Bonab, M., Sabetamal, H., and Bezuijen, A. 2014. Experimental study on foamed sandy soil for EPBM tunnelling. Advances in Railway Engineering, **2**(1): 27-40.

Horozov, T. S. 2008. Foams and foam films stabilized by solid particles. Current Opinion in Colloids and Interface Science, **13**(3): 134-140.

Hu, Q., Wang, S., Qu, T., Xu, T., Huang, S., and Wang, H. 2020. Effect of hydraulic gradient on the permeability characteristics of foam-conditioned sand for mechanized tunnelling. Tunnelling and Underground Space Technology, **99**, 103377.

Huang, S., Wang, S., Xu, C., Shi, Y., and Ye, F. 2019. Effect of grain gradation on the permeability characteristics of coarse-grained soil conditioned with foam for EPB shield tunneling. KSCE Journal of Civil Engineering, **23**(11): 4662-4674.

Hunter, T. N., Pugh, R. J., Franks, G. V., and Jameson, G. J. 2008. The role of particles in stabilising foams and emulsions. Advances in Colloid and Interface Science, **137**(2): 57-81.

ISO (International Organization for Standardization). 2008. Petroleum and natural gas industries-Drilling fluid materials-Specifications and tests: ISO 13500: 2008(E).

Jancsecz, S., Krause, R., and Langmaack, L. 1999. Advantages of soil conditioning in shield tunnelling: experiences of LRTS Izmir. Proc., Int. Congr. Challenges for the 21st Century, BalkemaRotterdam, pp. 865-875.

Kaptay, G. 2006. On the equation of the maximum capillary pressure induced by solid particles to stabilize emulsions and foams and on the emulsion stability diagrams. Colloids and Surfaces A Physicochemical and Engineering Aspects, **282**: 387-401.

Kenney, T. C., Veen, W. A., Swallow, M. A., and Sungaila, M. A. 1992. Hydraulic conductivity of compacted bentonite–sand mixtures. Canadian Geotechnical Journal, **29**(3): 364-374.

Langmaack, L., and Lee, K. 2016. Difficult ground conditions? Use the right chemicals! Chances–limits–requirements. Tunnelling and Underground Space Technology, **57**: 112-121.

Leonards, G. A., Huang, A. B., and Ramos, J. 1991. Piping and erosion tests at conner run dam. Journal of Geotechnical Engineering, American Society of Civil Engineers, **117**(1): 108-117.

Liu, P., Wang, S., Ge, L., Thewes, M., Yang, J., and Xia, Y. 2018. Changes of Atterberg limits and electrochemical behaviors of clays with dispersants as conditioning agents for EPB shield tunnelling. Tunnelling and Underground Space Technology, **73**(5): 244-251.

Louvet, N., Höhler, R., Pitois, O. (2010). Capture of particles in soft porous media. Physical Review E Statistical Nonlinear and Soft Matter Physics, **82**(4), 041405.

Ma, G., He, X., Jiang, X., Liu, H., Chu, J., and Xiao, Y. 2020. Strength and Permeability of Bentonite-Assisted Biocemented Coarse Sand [online]. Canadian Geotechnical Journal. https://doi.org/10.1139/cgj-2020-0045.

Mori, L., Alavi, E., and Mooney, M. 2017. Apparent density evaluation methods to assess the effectiveness of soil conditioning. Tunnelling and Underground Space Technology, **67**(8): 175-186.

Mori, L., Mooney, M., and Cha, M. 2018. Characterizing the influence of stress on foam conditioned sand for EPB tunneling. Tunnelling and Underground Space Technology, **71**: 454-465.

Olson, R.E., and Daniel D.E. 1981. Measurement of the hydraulic conductivity of fine-grained soils. American Society for Testing and Materials, pp. 18-64, West Conshohocken, PA.

Peila, D. 2014. Soil conditioning for EPB shield tunnelling. KSCE Journal of Civil Engineering, **18**(3): 831-836.

Peila, D., Borio, L., and Pelizza, S. 2011. The behaviour of a two-component backfilling grout used in a tunnel-boring machine. Acta Geotechnica Slovenica, **8**(1): 5-15.

Pitois, O., Lorenceau, E., Louvet, N., and Rouyer, F. 2009. Specific surface area model for foam permeability. Langmuir the Acs Journal of Surfaces and Colloids, **25**(1): 97-100.

Psomas, S. 2001. Properties of foam/sand mixtures for tunnelling applications. Degree of Master. Thesis. University of Oxford, UK.

Quebaud, S., Sibai, M., and Henry, J. 1998. Use of chemical foam for improvements in drilling by earth-pressure balanced shields in granular soils. Tunnelling and Underground Space Technology, **13**(2): 173-180.

Rouyer, F., Haffner, B., Louvet, N., Khidas, Y., and Pitois, O. 2014. Foam clogging. Soft Matter, **10** (36): 6990-6998.

Sivapullaiah, P. V., Sridharan, A., and Stalin, V. K. 2000. Hydraulic conductivity of bentonite-sand mixtures. Canadian Geotechnical Journal, **37**(2): 406-413.

Thewes, M., and Budach, C. 2010. Soil conditioning with foam during EPB tunnelling /. Konditionierung von Lockergesteinen bei Erddruckschilden. Geomechanik Und Tunnelbau, **3**(3): 256-267.

Vinai, R., Oggeri, C., and Peila, D. 2008. Soil conditioning of sand for EPB applications: a laboratory research. Tunnelling and Underground Space Technology, **23**(3): 308-317.

Wang S., Hu Q., Wang H., Thewes, M., Ge, L., Yang, J., and Liu, P. 2020. Permeability characteristics of poorly graded sand conditioned with foam in different conditioning states. Journal of Testing and Evaluation. https://doi.org/10.1520/JTE20190539.

Wang, S., Huang, S., Qiu, T., Yang, J., Zhong, J., and Hu, Q. 2020. Analytical study of the permeability of a foam-conditioned soil. International Journal of Geomechanics, **20**(8).

Wang, S., Huang, S., Zhong, J., Zhang, S., Hu, Q., Qu, T., and Ye, X. 2021. Permeability stability calculation model of foam-conditioned soil based on the permeability constant. International Journal for Numerical and Analytical Methods in Geomechanics, **45**(4): 540–559.

Wu, Y., Nazem, A., Meng, F., and Mooney, M.A. 2020. Experimental study on the stability of foam-conditioned sand under pressure in the EPBM chamber. Tunnelling and Underground Space Technology, **106**.

Xu, T., and Bezuijen, A. 2018a. Bentonite slurry infiltration into sand: filter cake formation under

various conditions. Géotechnique, **69**(12): 1095-1106.

Xu, T., and Bezuijen, A. 2018b. Pressure infiltration characteristics of bentonite slurry. Géotechnique, **69**(4): 364-368.

Xu, T., Bezuijen, A., and Thewes, M. 2021a. Pressure infiltration characteristics of foam for EPB shield tunnelling in saturated sand - part 1: 'clean' foam. Géotechnique. https://doi.org/10.1680/jgeot.19.P.187.

Xu, T., Bezuijen, A., and Thewes, M. 2021b. Pressure infiltration characteristics of foam for EPB shield tunnelling in saturated sand - Part 2: Soil-foam-mixture. Géotechnique. https://doi.org/10.1680/jgeot.19.P.188.

Zhao, G., Dai, C., Wen, D., and Fang, J. 2016. Stability mechanism of a novel three-phase foam by adding dispersed particle gel. Colloids and Surfaces A: Physicochemical and Engineering Aspects. **497**: 214-224.

LIST OF FIGURES

LIST OF TABLES

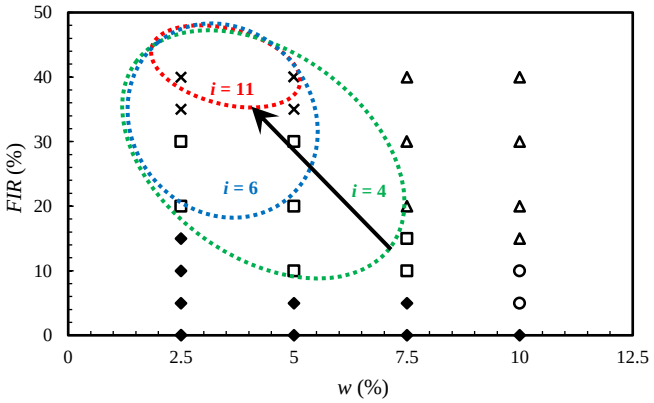

Fig. 1. Range of suitable conditioning parameters for permeabilities at different hydraulic gradients. ("□": Suitable conditioning without any water or foam bleeding, "◆": insufficient conditioning, "○": suitable conditioning but with water bleeding, "×": excessive conditioning with probable foam bleeding, "△": excessive conditioning with water bleeding) (Hu et al., 2020).

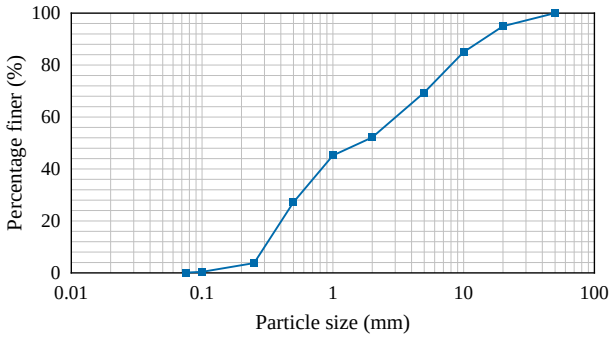

Fig. 2. Grain size distribution of the test sand.

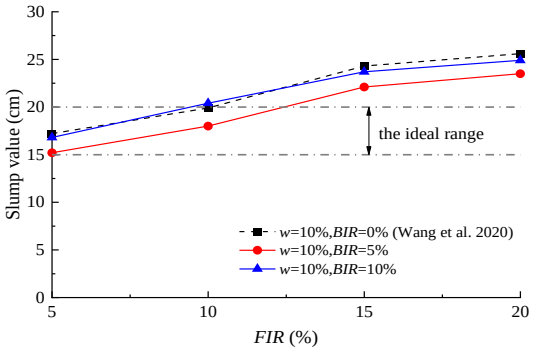

Fig. 3. Comparison of slump values between foam-bentonite slurry-conditioned sand and foam-conditioned sand.

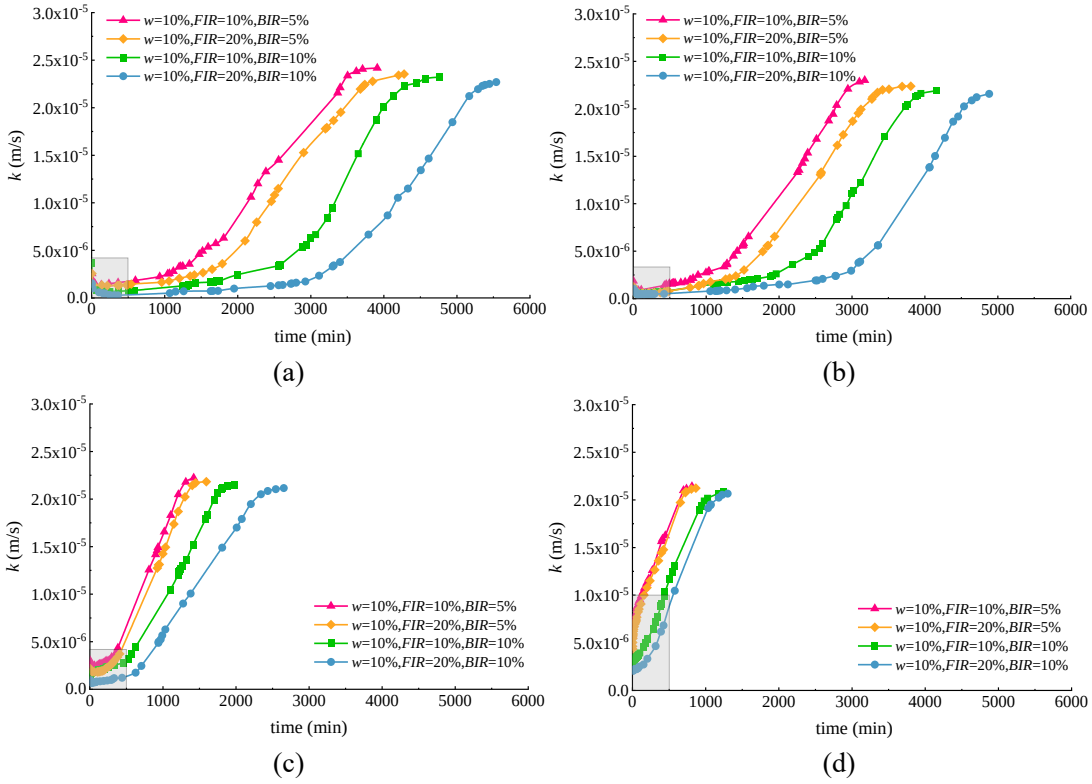

Fig. 4. Results of permeability tests with different hydrostatic pressure heads: (a) 1.9 m; (b) 2.9 m; (c) 5.6 m; (d) 9.6 m.

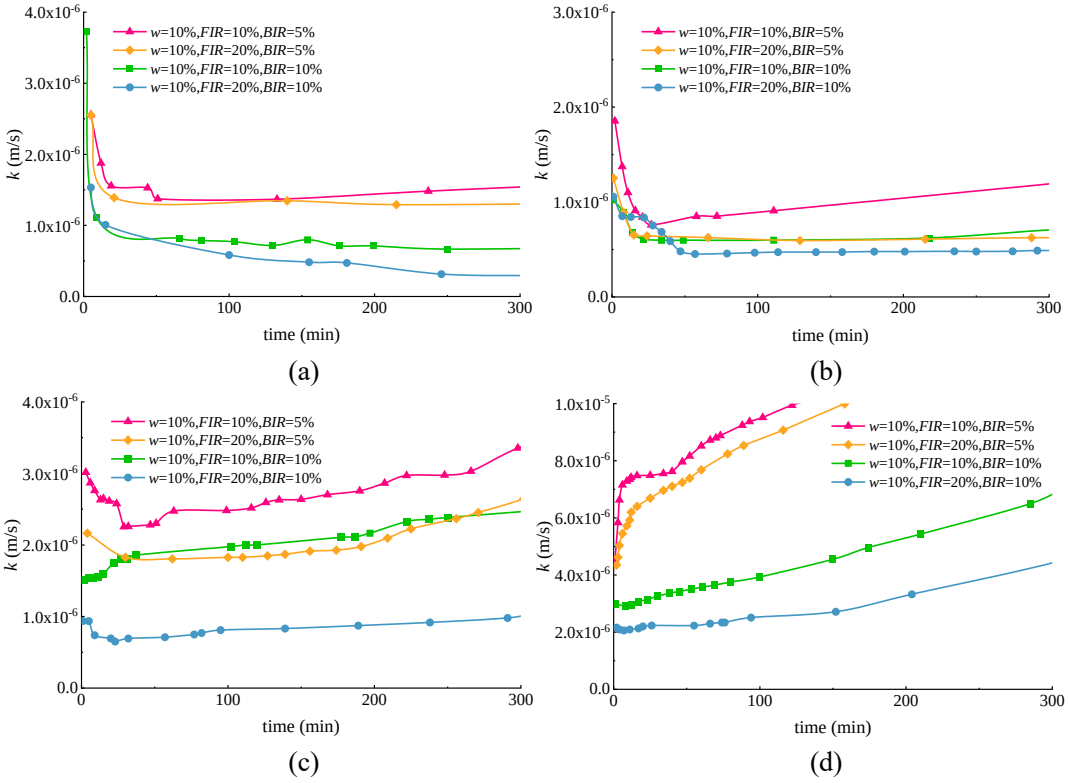

Fig. 5. Expanded inset of the early stage of the permeability coefficient: (a) 1.9 m; (b) 2.9 m; (c) 5.6 m; (d) 9.6 m.

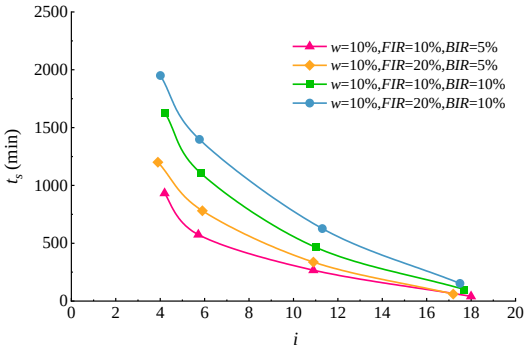

Fig. 6. Effect of the initial hydraulic gradient on the duration of the initial stable period.

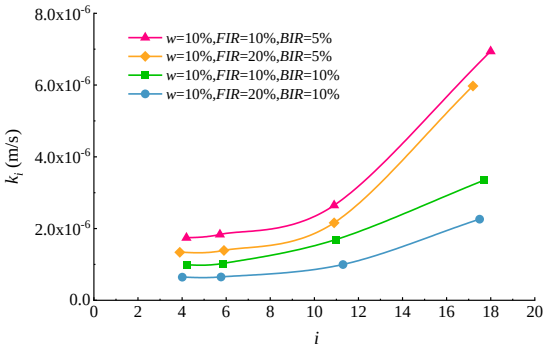

Fig. 7. Effect of the initial hydraulic gradient on the initial permeability coefficient.

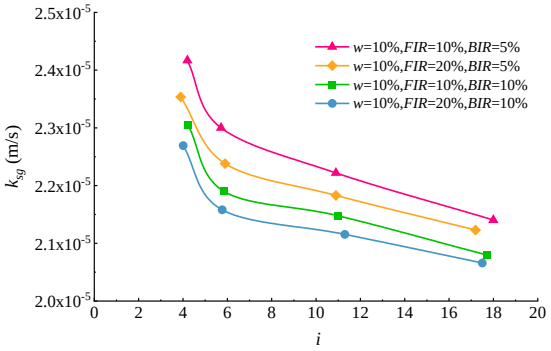

Fig. 8. Effect of the initial hydraulic gradient on the permeability coefficient in the slow growth period.

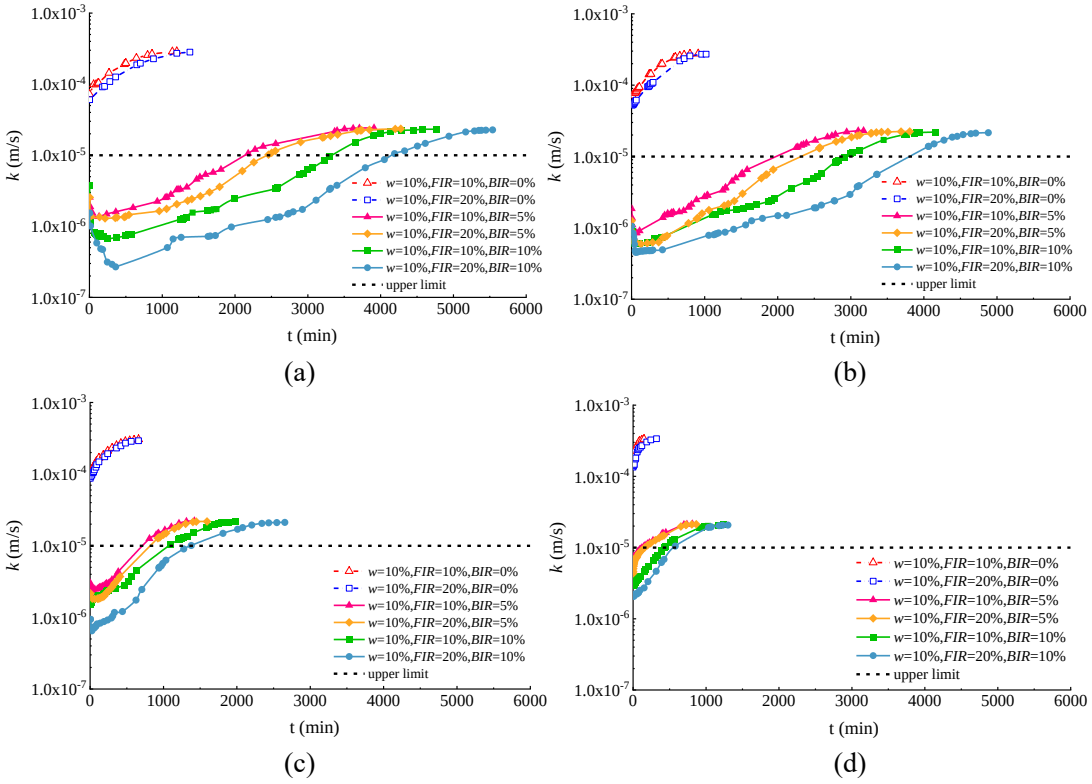

Fig. 9. Comparison of time-varying curves of the permeability coefficients of foam-bentonite slurry-conditioned sand and foam-conditioned sand under different hydrostatic pressure heads: (a) 1.9 m; (b) 2.9 m; (c) 5.6 m; (d) 9.6 m.

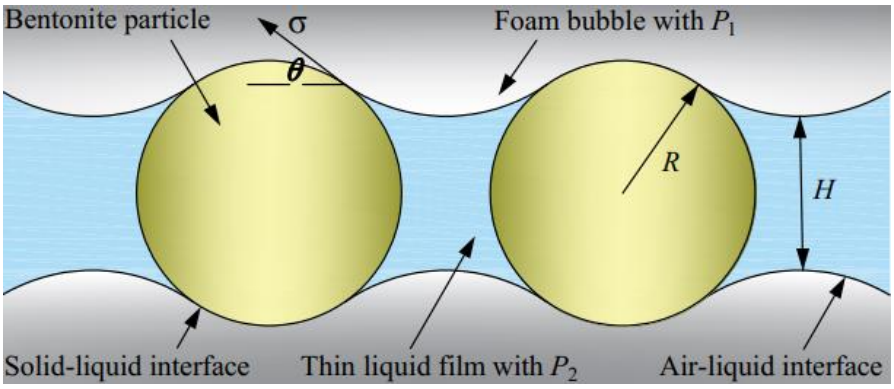

Fig. 10. Schematic diagram of the bentonite particle-stabilizing foam structure (modified from Kaptay, 2006).

Table 1 Chemical compositions of the foam agent.

Name	Percent	Function
Sodium dodecyl sulphate	1~1.5%	Anionic surfactant
Dodecyl ammonium chloride	3~3.5%	Cationic surfactant
Silicone oil	1~2%	Foam stabilizer
Water	93~94%	Solvent

Table 2 Mineral compositions of the sodium bentonite.

Mineral name	Chemical formula	Percent
Na-montmorillonite	$Na_{0.3}(Al,Mg)_2Si_4O_{10}(OH)_2$	48.8%
Ca-montmorillonite	$Ca_{0.2}(Al,Mg)_2Si_4O_{10}(OH)_2$	14.1%
Soda feldspar	$NaAlSi_3O_8$	28.3%
Microcline	$(K_{0.95}Na_{0.05})$ $(AlSi_3O_8)$	5.5%
Quartz	SiO_2	2.5%
Calcite	$CaCO_3$	0.8%

Table 3 Testing conditions of the permeability tests.

Water content (w)	Foam injection ratio (FIR)	Bentonite slurry injection ratio (BIR)	Conditioning states	Hydrostatic pressure head (P)	Initial hydraulic gradients (i)
10%	10%	5%	Suitable conditioning	1.9 m, 2.9 m, 5.6 m and 9.6 m	4.2, 5.8, 10.3, 17.0
		10%	Excessive but with no water bleeding		
	20%	5%	Excessive but with no water bleeding		
		10%	Excessive but with no water bleeding		